tvst

https://doi.org/10.1167/tvst.8.2.3

Article

Differential Artery–Vein Analysis Improves the Performance of OCTA Staging of Sickle Cell Retinopathy

Minhaj Alam[1], Jennifer I. Lim[2], Devrim Toslak[1,3], and Xincheng Yao[1,2]

[1] Department of Bioengineering, University of Illinois at Chicago, Chicago, IL, USA
[2] Department of Ophthalmology and Visual Sciences, University of Illinois at Chicago, Chicago, IL, USA
[3] Department of Ophthalmology, Antalya Training and Research Hospital, Antalya, Turkey

Correspondence: Xincheng Yao, Department of Bioengineering (MC 563), Department of Ophthalmology & Visual Sciences, University of Illinois at Chicago (UIC), Clinical Sciences North, Suite W103, Room 164D, 820 South Wood Street, Chicago, IL 60612, USA. xcy@uic.edu.

Received: 12 October 2018
Accepted: 30 January 2019
Published: 26 March 2019

Keywords: optical coherence tomography; sicke cell retinopathy; quantitative image analysis; retina; retinal vasculature

Citation: Alam M, Lim JI, Toslak D, Yao X. Differential artery–vein analysis improves the performance of OCTA staging of sickle cell retinopathy. Trans Vis Sci Tech. 2019;8(2):3, https://doi.org/10.1167/tvst.8.2.3

Purpose: We test if differential artery–vein analysis can increase the performance of optical coherence tomography angiography (OCTA) detection and classification of sickle cell retinopathy (SCR).

Method: This observational case series was conducted in a tertiary-retina practice. Color fundus and OCTA images were collected from 20 control and 48 SCR subjects. Fundus data were collected from fundus imaging devices, and SD-OCT and corresponding OCTA data were acquired using a spectral-domain OCT (SD-OCT) angiography system. For each patient, color fundus image-guided artery–vein classification was conducted in the OCTA image. Traditional mean blood vessel tortuosity (m-BVT) and mean blood vessel caliber (m-BVC) in OCTA images were quantified for control and SCR groups. Artery BVC (a-BVC), vein BVC (v-BVC), artery BVT (a-BVT), and vein BVT (v-BVT) were calculated; and then the artery–vein ratio of BVC (AVR–BVC) and artery–vein ratio of BVT (AVR–BVT) were quantified for comparative analysis.

Results: We evaluated 40 control and 85 SCR images in this study. The color fundus image-guided artery–vein classification had 97.02% accuracy for differentiating arteries and veins in OCTA. Differential artery–vein analysis provided significant improvement ($P < 0.05$) in detecting and classifying SCR stages compared to traditional mean blood vessel analysis. AVR–BVT and AVR–BVC showed significant ($P < 0.001$) correlation with SCR severity.

Conclusions: Differential artery–vein analysis can significantly improve the performance of OCTA detection and classification of SCR. AVR–BVT is the most sensitive feature that can classify control and mild SCR.

Translational Relevance: SCR and other retinovascular diseases result in changes to the caliber and tortuosity appearance of arteries and veins separately. Differential artery–vein analysis can improve the performance of SCR detection and stage classification.

Introduction

Sickle cell disease (SCD), one of the most common genetic disorders worldwide, is an inherited red blood cell disorder reported prevalently in Mediterranean regions, sub-Saharan Africa, the Middle East, and Southeast Asia.[1] In the United States, approximately 100,000 people are affected by SCD, according the American Society of Hematology reports in 2016.[2] Sickle cell retinopathy (SCR), a major ocular manifestation of SCD, typically results in vascular abnormality, foveal irregularity and vaso-occlusive ischemia. Early diagnosis in SCD patients with risk of SCR is essential for treatment evaluation and to prevent progression of retinopathy. In current clinical settings for SCR examination, the most commonly used imaging modalities are fundus and fluorescein angiography (FA) photography. However, these imaging modalities have limitation to reveal subclinical symptoms of SCR in SCD patients. As a new modality of optical coherence tomography (OCT),

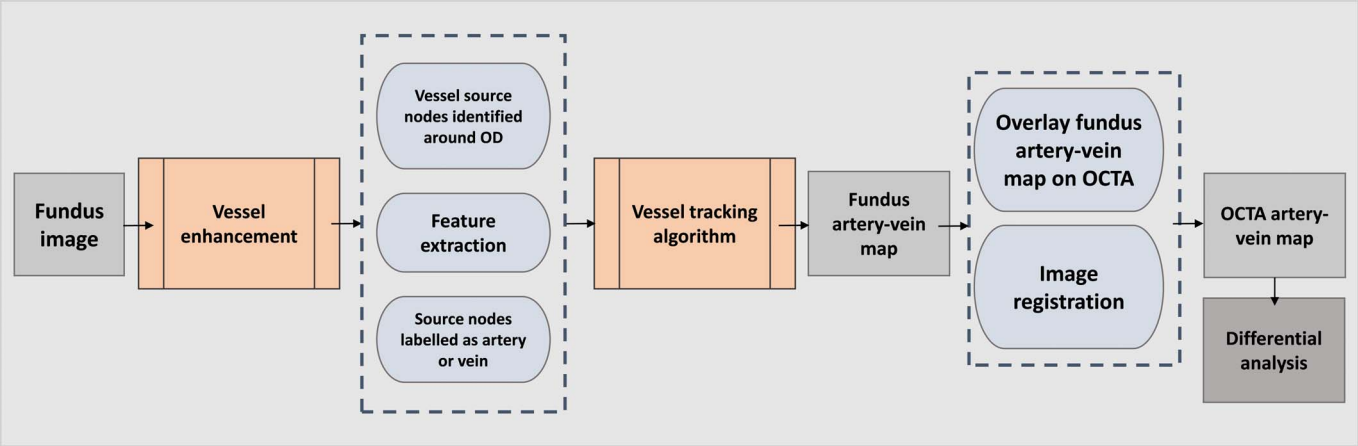

Figure 1. Flow diagram of color fundus image analysis-guided artery–vein classification in OCTA.

OCT angiography (OCTA) enables noninvasive observation of retinal vascular structures with spatial resolution at the individual capillary level.[3] OCTA has been explored extensively for quantitative assessment of retinal vascular distortions due to different eye diseases. Multiple OCTA features, such as blood vessel caliber (BVC), blood vessel tortuosity (BVT), vessel perimeter index (VPI), foveal avascular zone (FAZ) area, FAZ contour irregularity, and retinal vascular density, have been established for quantitative analysis and objective classification of SCR,[3,4] age-related macular degeneration (AMD),[5] diabetic retinopathy (DR),[6] and glaucoma.[7] However, quantifying the morphologic distortions in artery and veins separately remains challenging, but may provide better sensitivity in identifying disease progression.

Retinopathies have been known to affect arteries and veins differently. Focal arteriolar narrowing[8–10] and venous beading[11–14] have been reported in patients with hypertension, diabetes, and other eye diseases. For color fundus image analysis, artery–vein caliber ratio has been demonstrated as a predictor of retinopathy.[15–19] Differential analysis of arteries and veins holds promise to improve the performance of OCTA detection and classification of eye diseases. In our recent studies,[20,21] we reported fundus image-guided artery–vein differentiation as a feasible strategy to classify arteries and veins in OCTA of DR. We observed improved sensitivity in OCTA detection and classification of DR using two quantitative features, artery–vein ratios of BVC (AVR–BVC) and BVT (AVR–BVT). We tested if differential artery–vein analysis in OCTA can improve SCR detection and classification, and identified the most sensitive artery–vein features of SCR.

Methods

Study Protocol

This study was approved by the institutional review board of the University of Illinois at Chicago and followed the tenets of the Declaration of Helsinki. SCR patients were recruited from the retina clinic of the University of Illinois at Chicago. The complete anterior and dilated posterior segment was examined (JIL). SCR stages were graded (stage I–V, from mild to severe) according to the Goldberg classification. We included stages II and III SCR patients in our study as stage I OCTA data were not available and stage IV OCTA images were not reliable due to distortions caused by vessel proliferation and hemorrhages. For simplifying the classification process, we defined stages II and III as mild and severe stage SCR, respectively. The database consisted of 20 control and 48 SCR patients (30 mild and 18 severe SCR); OCTA images were captured from both eyes of each subject. Control data were from healthy volunteers who gave informed consent for fundus photography and OCTA imaging. All subjects with previous vitreous surgery or prior intravitreal injections were excluded. Patients also were excluded if they were diagnosed with other eye diseases or had significant pathologic features in their retina such as macular edema, vein occlusions or epiretinal membranes.

Figure 1 illustrates core steps of the color fundus image-guided artery–vein classification in OCTA. Color fundus images were captured using a fundus camera (Cirrus-800; Zeiss, Oberkochen, Germany and Pictor nonmydriatic retinal camera; Volk, Mentor,

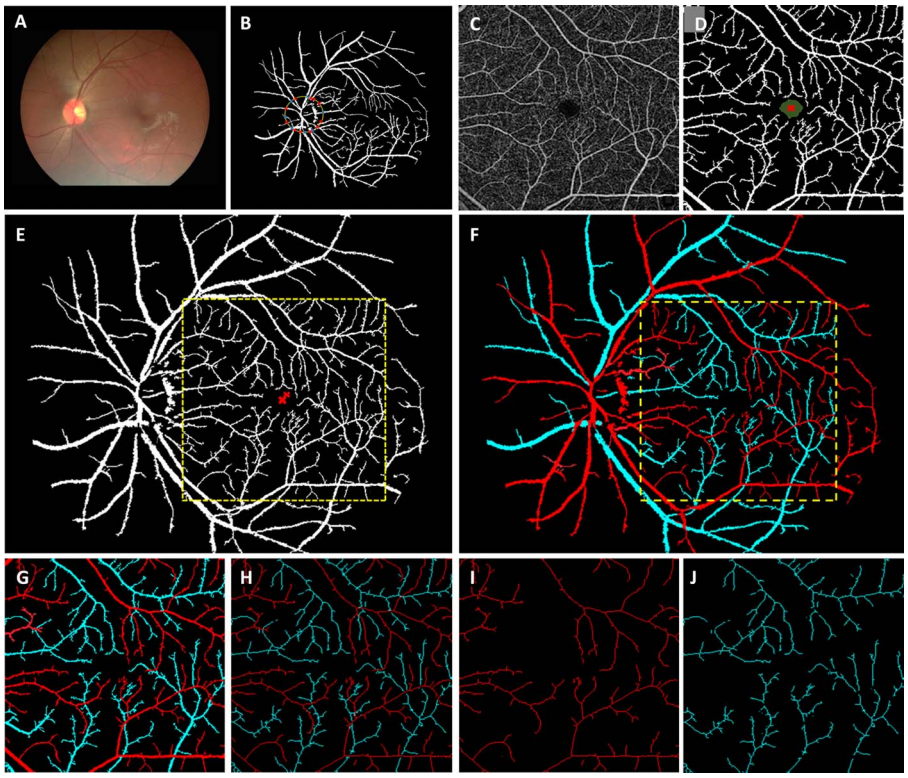

Figure 2. (A) Color fundus image. (B) Segmented vessel map. (C) OCTA image. (D) Segmented vessel map from OCTA. (E) OCTA vessel map registered with fundus vessel map. (F) Fundus artery–vein map was used to guide artery–vein differentiation in OCTA image. (G) Artery–vein map in OCTA. (H) Artery–vein skeleton map in OCTA. (I) Artery–skeleton map. (J) Vein–skeleton map. The vessel and skeleton maps are used to measure BVC and BVT separately for arteries and veins.

OH) with a 30° to 45° field of view (FOV) and an image resolution of 2392 × 2048 pixels. SD-OCT and corresponding OCTA data were acquired using an Angiovue SD-OCT angiography system (Optovue, Fremont, CA), consisting of a 70-KHz A-scan rate, and axial and lateral resolutions of approximately 5 and 15 μm, respectively. All analyzed OCTA images were 6 × 6 mm scans. We maintained a general quality standard for including fundus and OCTA images in our database. Two separate eye specialists qualitatively examined all images in the database. Fundus images with irregular illumination and severe light saturation in the parafoveal retina, or that did not included optic disk and foveal region of the retina, and OCTA images affected with severe motion artifact were excluded. Projection artifacts in OCTA images were not a significant factor for this study, because we only used the superficial retinal layer, which includes 80% of the ganglion cell complex (from the inner plexiform layer to the border of the inner nuclear plexus). The fundus and OCTA images were exported from respective devices and custom-developed MATLAB (Mathworks, Natick, MA) procedures with graphical user interface (GUI) were used for further image analysis, feature extraction, and image classification.

Figure 2 illustrates key procedures of the color fundus image analysis guided artery–vein classification. The representative color fundus (Fig. 2A) and OCTA (Fig. 2C) images were acquired from a control subject. Briefly, optical density ratio (ODR) analysis and blood vessel tracking algorithms were combined to identify artery–vein in color fundus images.[22] For the OCTA vessel map (Fig. 2D), a Hessian based multiscale Frangi filter was used to enhance the vascular flow information. The Frangi filtering method evaluates the Eigen vectors of the Hessian matrices of the OCTA image and computes the likeliness of any pixel of the OCTA image to be a vascular structure. Adaptive thresholding and morphologic functions were implemented further for cleaning the OCTA vessel map and removing small capillary branches and mesh structures that were not suitable for the vessel tracking algorithm. The

Table 1. Demographics of Control and SCR Subjects

	Control	Sickle Cell Retinopathy	
		Mild SCR	Severe SCR
Number of subjects	20	30	18
Sex (male)	12	17	11
Number of images	40	50	35
Age (mean ± SD), years	42 ± 9.7	51 ± 11.52	59.73 ± 8.26
Age, range, years	25–71	28–71	46–75

extracted vessel maps from the OCTA images had an average area of 18.25% (standard deviation [SD], 2.9; range, 14.39%–24.58%). The fundus artery–vein map was used to register arteries and veins in the OCTA vessel map (Figs. 2E, 2F) using a geometric-affine based image registration method.[23] Technical details of the artery–vein classification process have been reported previously.[20,24] The artery–vein classification performance in fundus and OCTA images was validated using ground truths prepared by two experienced ophthalmologists (JIL and DT). Based on the fundus image-guided artery–vein differentiation, quantitative analysis of control and SCR OCTA images was performed. Traditional mean (m) BVC and m-BVT without artery–vein differentiation in OCTA were first quantified for control and SCR groups. Then, artery BVC (a-BVC), vein BVC (v-BVC), artery BVT (a-BVT), and vein BVT (v-BVT) were quantified for comparative evaluation. The BVC was defined as,

$$BVC = \frac{Vascular\_area}{Vascular\_length} \quad (1)$$

where the vascular area and length are calculated from the corresponding vessel (Fig. 2G) and skeleton (Fig. 2H) maps, respectively. Average BVT was defined as,

$$BVT = \sum \frac{Geodesic\_distance}{Euclidean\_distance} \quad (2)$$

where Geodesic distance represents the curve length of individual capillary (real length), while Euclidian distance represents an imaginary straight length between two endpoints of the capillary branch.

After measuring the BVC and BVT features, artery–vein ratios of BVC and BVT were calculated as AVR–BVC = a-BVC/v-BVC and AVR–BVT = a-BVT/v-BVT, respectively. Further details of the methodology of feature calculation were reported in our previous publication.[20]

Statistical Analyses

We used a 1-way, multilabel analysis of variance (ANOVA) with Bonferroni's correction to compare the difference of mean values of these vascular parameters among multiple groups (statistical significance defined as $P < 0.05$). One versus one comparison of these parameters between the control and SCR (mild/severe) stages was performed by the 2-sample Student's t-test. We used χ^2 tests to compare the distribution of sex and hypertension among different groups, age distribution was compared using ANOVA. The repeatability of AVR–BVC and AVR–BVT features was tested using intraclass correlation coefficients (ICC) from 2-repeat measurements. For all measurements, statistical significance was defined as $P < 0.05$.

Results

Images from 20 control subjects and 48 SCR patients, including 30 mild (stage II), and 18 severe (stage III) stages, were used for this study. The detailed patient demographic data are shown in Table 1.

There were no statistically significant differences between control and SCR groups with respect to distribution of age or sex (χ^2, $P > 0.12$). We validated the artery–vein classification in fundus and OCTA images with ground truths prepared by retina specialists (JIL and DT). The algorithm demonstrated 97.16% and 95.83% accuracy in identifying blood vessels as artery and vein, respectively, based upon the OCTA images. We observed 95.47% sensitivity and 96.12% specificity for artery identification, and 94.86% sensitivity and 96.59% specificity for vein identification. Figure 3 illustrates comparative fundus, OCTA, and artery–vein maps of representative control (Fig. 3A), mild (Fig. 3B), and severe (Fig. 3C) SCR groups.

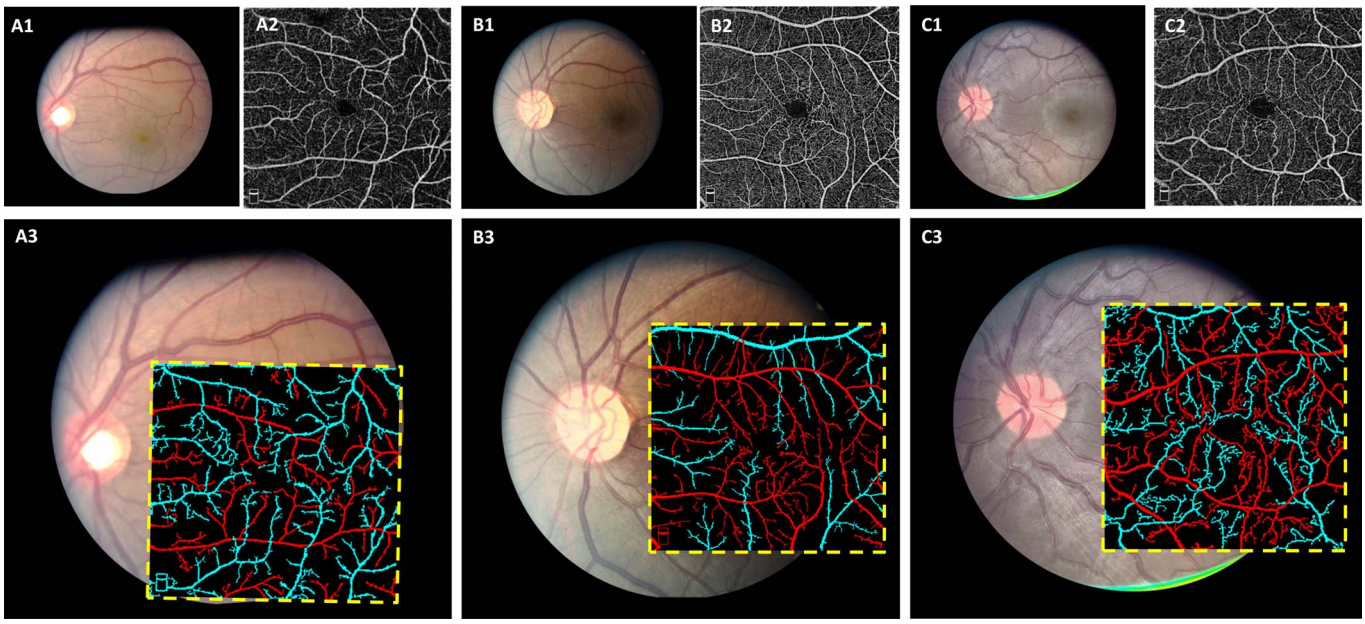

Figure 3. Representative artery–vein classification results from control (A), mild SCR (B), and severe SCR (C) groups. (A1–C1) Fundus images. (A2–C2) OCTA images. (A3–C3) OCTA artery–vein maps overlaid on corresponding fundus images.

Quantitative analysis of control and SCR OCTAs is summarized in Figure 4A and 4B. We compared the sensitivity of AVR–BVC and AVR–BVT with m-BVC and m-BVT respectively. We also verified if AVR–BVC and AVR–BVT improved the feature sensitivity for control versus SCR OCTAs compared to a-BVC, a-BVT or v-BVC, v-BVT.

For BVT analysis (Fig. 4A), tortuosity measured in the whole vessel map, m-BVT increased as SCR stage progressed. We observed 10.3% and 15% increases for mild and severe SCR, respectively, compared to control data. As shown in Figure 4A3, m-BVT values were not significant to differentiate the control and two SCR groups (ANOVA, $P = 0.09$). The m-BVT change was relatively small due to the opposite polarity of a-BVT and v-BVT. A-BVT did not show any significant changes among the groups, whereas the v-BVT primarily contributed to the morphologic distortions in SCR patients. For a-BVT (Fig. 4A1), 2.09% and 1.38% decreases were observed for control versus mild and control versus severe SCR OCTAs, respectively. On the contrary, we observed 17.45% and 28.5% increases in v-BVT in mild and severe SCR groups, respectively, compared to the control group. This also reflected the change in AVR–BVT. In comparison with m-BVT assessment, AVR–BVT showed increased sensitivity (Fig. 4A4). AVR–BVT revealed 12.22% and 21.11% decreases for mild and severe SCR OCTAs compared to control OCTA data (Student's t-test, $P < 0.001$ for all three cases). V-BVT and AVR–BVT also showed excellent performance to differentiate these three groups (control and two SCR groups; ANOVA, $P = 0.003$; Fig. 4A4) and to differentiate control and mild SCR groups (Student's t-test, $P < 0.002$). This promises a unique biomarker for detecting early onset of SCR in sickle cell patients.

For BVC analysis (Fig. 4B), differential features (v-BVC and AVR–BVC) improved the sensitivity significantly compared to m-BVC. The a-BVC (Fig. 4B1) demonstrated small changes between control and SCR groups (1.9% and 7.26% decrease for control vs. mild SCR, and control vs. severe SCR), but v-BVC (Fig. 4B2) increased as SCR stage progressed (10.8 and 16.8% increases for control vs. mild SCR, and control vs. severe SCR). The m-BVC demonstrated limited change in control and SCR groups (0.72% and, 2.53% increases in mild and severe SCR groups, compared to control; Fig. 4B3). For AVR–BVC, 11.5% and 20.6% decreases were observed for control versus mild, and control versus severe SCR (moderately significant, $P < 0.04$ for all cases) eyes (Fig. 4B4). V-BVC and concurrently AVR–BVC could distinguish mild and severe SCR stages as well (Student's t-test, $P = 0.041$). Intergroup change for these two features also was statistically significant (ANOVA, $P = 0.02$).

We measured Pearson's correlation coefficients (r_s) to analyze the relationship among OCTA features and their correlation with SCR severity. AVR–BVT and

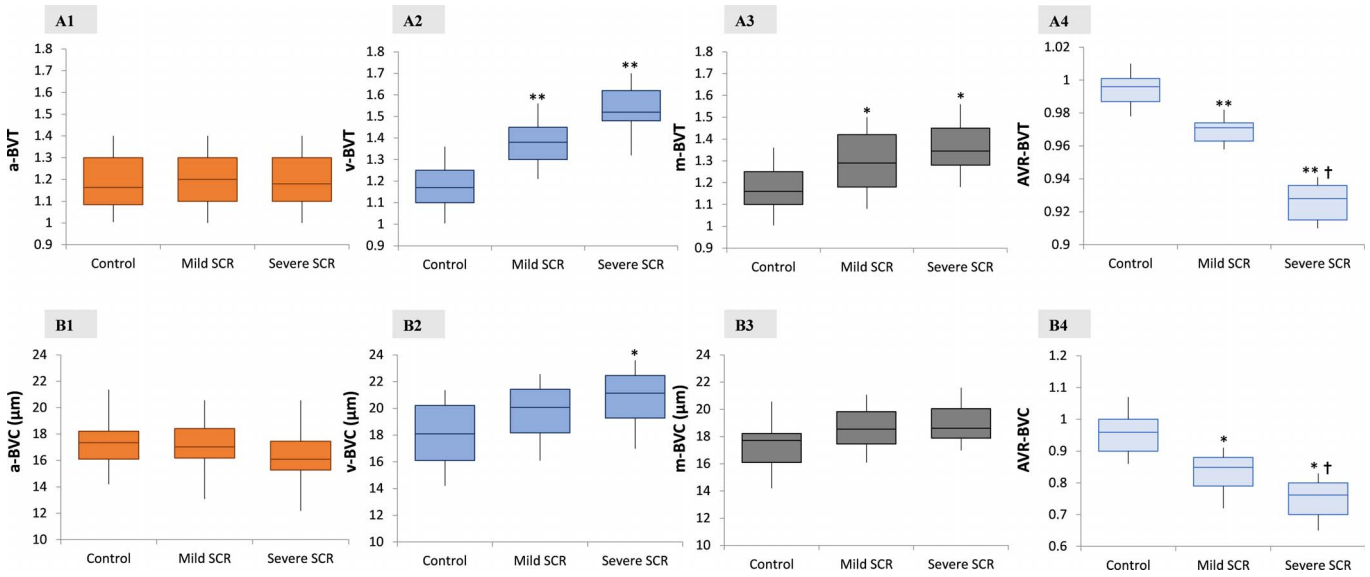

Figure 4. BVT and BVC changes between control and SCR patients. (A1–A4) a-BVT, v-BVT, m-BVT and AVR–BVT differences between control and SCR stages. (B1–B4) a-BVC, v-BVC, m-BVC and AVR–BVC differences between control and SCR stages. *Moderately significant change compared to control ($P < 0.05$). **Highly significant change compared to control ($P < 0.001$). †Moderately significant change between two SCR stages.

AVR–BVC showed significant negative correlation with SCR stages. ($r_s = -0.416, -0.573$ respectively; all $P < 0.001$). AVR–BVT and AVR–BVC also had a negative correlation with v-BVT and v-BVC ($r_s = -0.220, -0.194$, and $P = 0.008, 0.009$ respectively).

Discussion

We conducted differential artery–vein analysis to evaluate microvascular distortions in OCTA of SCR. Color fundus image-guided artery–vein classification was implemented to differentiate arteries and veins in SCR OCTA images, with 97.02% accuracy. Two quantitative features, AVR–BVT and AVR–BVC, then were used to identify control versus SCR subjects and mild versus severe SCR stages. As the vessel tortuosity and caliber in the artery and vein can be affected in different ways by SCR, the differential artery–vein analysis improved the performance and sensitivity of OCTA classification. Especially, for m-BVC, significant differences in control and SCR OCTAs were not observed due to opposite polarities of a-BVC and v-BVC (i.e., arterial narrowing and venous widening). In contrast, the differential artery–vein analysis, AVR–BVC and AVR–BVT, provided enhanced sensitivity to differentiate the control and SCR stages. V-BVT and AVR–BVT were demonstrated to reliably differentiate control and mild SCR stages. In case of AVR–BVT and AVR–BVC, we observed that the vein morphology contributed more to the changes and vascular distortions in diseased retinas (mild and severe SCR).

In our previous OCTA study of SCR,[3] we observed morphologic changes in mild and severe SCR patients. We observed increased BVT and BVC compared to control subjects. However, performance of the m-BVT or m-BVC was somewhat limited as the artery and vein were affected differently in the retinopathy. For SCR, veins were observed to be more dilated and tortuous.[3,25,26] For example, Condon et. al.[26] reported that approximately 72% of the SCR patients showed tortuosity change only in veins. Therefore, differential analysis of vessel tortuosity and caliber changes promises a more robust approach to identify vascular distortions in SCD patients. We recently demonstrated differential artery–vein classification in OCTA of DR,[20] and demonstrated AVR–BVT and AVR–BVC as two quantitative features for objective staging of DR patients. In our study, we adapted a similar strategy to test if the differential artery–vein analysis in SCR can improve the performance of quantitative OCTA analysis. In case of BVT, we observed increased v-BVT with progression of disease stage, while a-BVT did not show significant change. Compared to control, mild and severe stages had significantly increased v-BVT. Reflecting the changes in v-BVT, AVR–BVT also is a balanced feature, showing significant differences when com-

pared to control and also among mild and severe SCR stages. A similar trend was observed in BVC analysis. A-BVC and m-BVC demonstrated limited change with disease progression, while v-BVC only showed a significant change in severe stage SCR. V-BVC and AVR–BVC could identify mild and severe SCR from control data and also from each other. This result also was validated using Pearson's correlation test, which showed that the AVR–BVT and AVR–BVC demonstrated significant negative correlation with SCR stages.

One limitation of this study was the exclusion of microcapillary structures in the foveal region. They were not included in the 6 mm FOV vascular map due to the limitation of our vessel tracking algorithm. In future studies, we plan to use higher resolution 3×3 mm FOV OCTAs for vessel tracking and possibly include the small capillary structures near the fovea for a more detailed analysis of retinal artery and vein vasculature. We also plan to include a larger number of OCTA data for further study on classification of SCR stages.

In conclusion, color fundus image-guided artery–vein classification enabled quantitative analysis of arteries and veins in OCTAs from SCR patients. Differential artery–vein analysis improves the sensitivity of SCR detection and classification. V-BVT and AVR–BVT were demonstrated as sensitive features to reliably differentiate control and mild SCR stages, promising unique biomarkers for early detection of SCR.

Acknowledgments

Supported by National Institutes of Health (NIH, Bethesda, MD, USA) Grants R01 EY023522, R01 EY024628, P30 EY001792; an unrestricted grant from Research to Prevent Blindness; Richard and Loan Hill endowment; and Marion H. Schenk Chair endowment.

Disclosure: **M. Alam**, P; **J.I. Lim**, None; **D. Toslak**, None; **X. Yao**, P

References

1. El-Hazmi MA, Al-Hazmi AM, Warsy AS. Sickle cell disease in Middle East Arab countries. *Ind J Med Res*. 2011;134:597.
2. American Society of Hematology: State of Sickle Cell Disease, 2016 report
3. Alam M, Thapa D, Lim JI, Cao D, Yao X. Quantitative characteristics of sickle cell retinopathy in optical coherence tomography angiography. *Biomed Opt Exp*. 2017;8:1741–1753.
4. Alam M, Thapa D, Lim JI, Cao D, Yao X. Computer-aided classification of sickle cell retinopathy using quantitative features in optical coherence tomography angiography. *Biomed Opt Exp*. 2017;8:4206–4216.
5. Palejwala NV, Jia Y, Gao SS, et al. Detection of non-exudative choroidal neovascularization in age-related macular degeneration with optical coherence tomography angiography. *Retina*. 2015;35:2204.
6. Kim AY, Chu Z, Shahidzadeh A, Wang RK, Puliafito CA, Kashani AH. Quantifying microvascular density and morphology in diabetic retinopathy using spectral-domain optical coherence tomography angiography. *Invest Ophthalmol Vis Sci*. 2016;57:OCT362–370.
7. Holló G. Vessel density calculated from OCT angiography in 3 peripapillary sectors in normal, ocular hypertensive, and glaucoma eyes. *Eur J Ophthalmol*. 2016;26:e42–45.
8. Pedersen L, Jeppesen P, Knudsen ST, Poulsen PL, Bek T. Improvement of mild retinopathy in type 2 diabetic patients correlates with narrowing of retinal arterioles. A prospective observational study. *Graef's Arch Clin Exp Ophthalmol*. 2014; 252:1561–1567.
9. Klein R, Klein BE, Moss SE, Wang Q. Hypertension and retinopathy, arteriolar narrowing, and arteriovenous nicking in a population. *Arch Ophthalmol*. 1994;112:92–98.
10. Cheung N, Bluemke DA, Klein R, et al. Retinal arteriolar narrowing and left ventricular remodeling: the multi-ethnic study of atherosclerosis. *J Am Coll Cardiol*. 2007;50:48–55.
11. Fonseca RA, Dantas MA. Retinal venous beading associated with recurrent branch vein occlusion. *Canad J Ophthalmol*. 2002;37:182–183.
12. Gregson PH, Shen Z, Scott RC, Kozousek V. Automated grading of venous beading. *Comput Biomed Res*. 1995;28:291–304.
13. Kozousek V, Shen Z, Gregson P, Scott RC. Automated detection and quantification of venous beading using Fourier analysis. *Canad J Ophthalmol*. 1992;27:288–294.
14. Piguet B, Gross-Jendroska M, Holz FG, Bird AC. Inherited venous beading. *Eye*. 1994;8(Pt 1): 84–88.

15. Niemeijer M, Xu X, Dumitrescu AV, et al. Automated measurement of the arteriolar-to-venular width ratio in digital color fundus photographs. *IEEE Trans Med Imag*. 2011;30:1941–1950.
16. Hubbard LD, Brothers RJ, King WN, et al. Methods for evaluation of retinal microvascular abnormalities associated with hypertension/sclerosis in the Atherosclerosis Risk in Communities Study. *Ophthalmology*. 1999;106:2269–2280.
17. Ikram MK, Witteman JC, Vingerling JR, Breteler MM, Hofman A, de Jong PT. Retinal vessel diameters and risk of hypertension. *Hypertension*. 2006;47:189–194.
18. Liew G, Wong TY, Mitchell P, Cheung N, Wang JJ. Retinopathy predicts coronary heart disease mortality. *Heart*. 2009;95:391–394.
19. Wong TY, Knudtson MD, Klein R, Klein BE, Meuer SM, Hubbard LD. Computer-assisted measurement of retinal vessel diameters in the Beaver Dam Eye Study: methodology, correlation between eyes, and effect of refractive errors. *Ophthalmology*. 2004;111:1183–1190.
20. Alam M, Toslak D, Lim JI, Yao X. Color fundus image guided artery-vein differentiation in optical coherence tomography angiography. *Invest Ophthalmol Vis Sci*. 2018;59:4953–4962.
21. Son T, Alam M, Liu C, Toslak D, Yao X. Artery and vein differentiation in retinal optical coherence tomography angiography of macular region. *Ophthalmic Technologies XXIX*. International Society for Optics and Photonics. 2019;10858.
22. Alam M, Son T, Toslak D, Lim JI, Yao X. Combining optical density ratio and blood vessel tracking for automated artery-vein classification and quantitative analysis in color fundus images *Trans Vis Sci Tech*. 2018;7:23.
23. Thevenaz P, Ruttimann UE, Unser M. A pyramid approach to subpixel registration based on intensity. *IEEE Trans Imag Proc*. 1998;7:27–41.
24. Alam M, Son T, Toslak D, Lim JI, Yao X. Combining ODR and blood vessel tracking for artery–vein classification and analysis in color fundus images. *Transl Vis Sci Tech*. 2018;7:23–23.
25. Fadugbagbe A, Gurgel R, Mendonça C, Cipolotti R, Dos Santos A, Cuevas L. Ocular manifestations of sickle cell disease. *Ann Trop Paediatr*. 2010;30:19–26.
26. Condon PI, Serjeant GR. Ocular findings in homozygous sickle-cell anemia in Jamaica. *Am J Ophthalmol*. 1972;73:533–543.